ResearchGate

See discussions, stats, and author profiles for this publication at: https://www.researchgate.net/publication/278586697

Liquid-Phase Vibrational Strong Coupling

ARTICLE *in* JOURNAL OF PHYSICAL CHEMISTRY LETTERS · JANUARY 2015

Impact Factor: 7.46

READS

15

1 AUTHOR:

Jino George

University of Strasbourg

12 PUBLICATIONS **132** CITATIONS

SEE PROFILE

Available from: Jino George
Retrieved on: 30 January 2016

THE JOURNAL OF PHYSICAL CHEMISTRY Letters

Letter

pubs.acs.org/JPCL

Liquid-Phase Vibrational Strong Coupling

Jino George, Atef Shalabney, James A. Hutchison, Cyriaque Genet, and Thomas W. Ebbesen*

ISIS & icFRC, Université de Strasbourg and CNRS, 8 allée Gaspard Monge, Strasbourg 67000, France

ABSTRACT: Light-matter strong coupling involving ground-state molecular vibrations is investigated for the first time in the liquid phase for a set of molecules placed in microcavities. By tuning the cavities, one or more vibrational modes can be coupled in parallel or in series, inducing a change in the vibrational frequencies of the bonds. These findings are of fundamental importance to fully develop light-matter strong coupling for applications in molecular and material sciences.

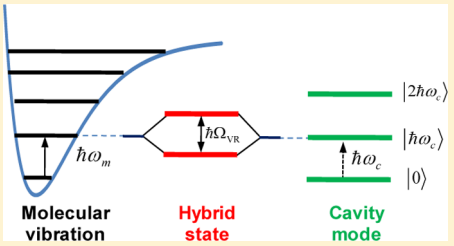

Through the formation of hybrid light-matter states, light-matter strong coupling offers exciting new possibilities for molecular and material sciences[1−41] by inducing significant changes in their properties. So far this has been mainly demonstrated by strongly coupling electronic transitions to the confined electromagnetic field of a cavity or a plasmonic structure. For instance, the rate of a photochemical isomerization reaction and the work function and conductivity of organic semiconductors can be modified under strong coupling.[14−18]

Strong coupling is not limited to electronic transitions.[10] In particular, the coupling of light to a vibrational transition should be very promising for molecular science because it is potentially a simple way to modify a given chemical bond because it generates two new vibrational modes (strictly speaking vibrational polaritonic states) separated by the Rabi energy, as illustrated in Figure 1a. This should, in turn, soften the bond because the vibrational frequency $\omega_v \propto (f/\mu)^{1/2}$, where μ is the reduced mass of the atoms involved and f is the bond strength. We expect that this might modify the Morse potential of the ground state and therefore the associated chemistry and chemical properties. In view of the long wavelengths of vibrational transition, the strong coupling can be achieved in cavities with micrometer dimensions, further faciliting the application to molecular science such as the integration into microfluidic cells. Finally, as we detail later, light-matter strong coupling can occur even in the dark due to the zero-point fluctuations of the cavity, which interact with those of the vibrational transitions.

Recently we reported the very first example of vibrational strong coupling (VSC)[10] by placing a solid polymer film between two mirrors forming a Fabry−Perot (FP) cavity tuned to the C═O stretching band at 1740 cm^{-1}, resulting in a Rabi splitting of 167 cm^{-1}. For VSC to be useful to molecular science, a number of other issues must be solved. First of all, the molecular sample should be coupled in the liquid state to be able to investigate various chemical processes. Second, there may be fundamental differences between SC in the liquid and solid states, and one might anticipate, for instance, that rapid reorientation in solution could increase dephasing rate. Third, there is a fundamental question of whether strong coupling of an ensemble of N oscillators, which boosts the Rabi splitting by $\sqrt{N}$ through the formation of a collective polaritonic state, actually perturbs the energy levels of the other states of the molecules involved by the same quantity. It is sometimes argued that on the scale of each molecule, the effective Rabi splitting is the observed collective Rabi splitting divided by $\sqrt{N}$. If this was the case the effect of the strong coupling on individual molecules would be negligible and it would be of no interest to chemistry. Experimental evidence indicates that this view is not correct because significant changes in chemical and material properties are observed.[14−18]

Here we provide insight into these issues. We report, for the first time in the liquid state, the VSC of different molecules and functional groups and show that one can strongly couple one or more bonds of a given molecule by placing them in flow-cell Fabry−Perot cavities. Because vibrational modes are themselves sometimes coupled, we looked whether VSC induces a shift in a neighboring bond that is not directly strongly coupled. However, with our experimental resolution and the systems under consideration, we could not detect such shift.

Before showing the results, it is important to recall the theoretical framework of strong coupling, as we explained previously.[13] The Rabi splitting ($\hbar\Omega_R$) is proportional to the scalar product of the electromagnetic field amplitude ($E\rightharpoonup$) at the energy $\hbar\omega$ of the optical resonance and the material transition dipole moment ($d\rightharpoonup$), which in the absence of dissipation is given by

$$\hbar\Omega_R = 2\vec{E}\cdot\vec{d} \times \sqrt{n_{ph}+1} = 2\sqrt{\frac{\hbar\omega}{2\varepsilon_0 V}}\, d \times \sqrt{n_{ph}+1} \quad (1)$$

where ε_0 is the vacuum permittivity and n_{ph} is the number of photons involved in the coupling process. As already pointed out, eq 1 shows that the splitting can still occur even in the absence of real photons ($n_{ph} = 0$) due to interaction of the

Received: January 29, 2015
Accepted: March 5, 2015
Published: March 5, 2015

 © 2015 American Chemical Society

DOI: 10.1021/acs.jpclett.5b00204
J. Phys. Chem. Lett. 2015, 6, 1027−1031

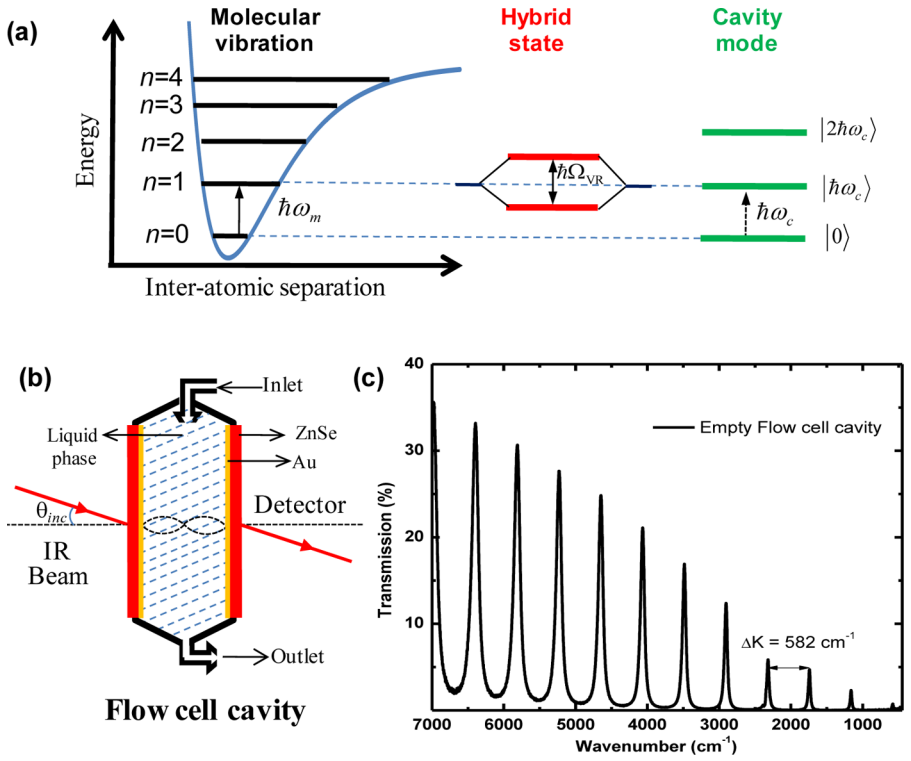

Figure 1. (a) Schematic illustration of the light matter coupling between one vibrational transition and a cavity mode resulting in the Rabi splitting $\hbar\Omega_{VR}$. (b) Illustration of the flow-cell Fabry–Perot cavity. (c) Measured optical resonances of an empty cavity having of length 8.6 μm.

vibrational transition dipole and the cavity mode through zero-point energy fluctuations. This residual splitting is known as the vacuum Rabi splitting ($\hbar\Omega_{VR}$). All of the experiments reported here are done in this regime. In addition, the Rabi splitting increases as the square root of the molecular concentration, C, because $\hbar\Omega_{VR} \propto (N/V)^{1/2} = \sqrt{C}$, where N is the number of coupled molecules in the mode volume, V.

Figure 1b illustrates the IR flow-cell Fabry–Perot cavity, in which the experiments were undertaken. The windows are composed of ZnSe coated with 10 nm of Au. An example of the transmission spectrum showing the various optical, or Fabry–Perot, modes are given in Figure 1c, typical for a cavity path length of 8.6 μm and Q factor of 63. The decreasing peak intensities at short wavenumbers are due to the evolution of the dielectric constants of the Au mirrors in this spectral region.

The IR absorption spectra (black curves) of three different molecules are shown in Figure 2, together with those under VSC (red curves). The first example is that of diphenyl phosphoryl azide (DPPA), which displays a number of sharp vibrational absorption peaks (Figure 2a). Of particular interest is the strong and isolated N═N═N stretching mode at 2169 cm^{-1}. The cavity was made to have one of its resonances be isoenergetic with this peak, resulting in the formation of two new hybrid modes on either side of the original frequency. The vacuum Rabi splitting is found to be 127 cm^{-1} , which is larger than both the full width at half-maximum (fwhm) of the FP cavity mode (43 cm^{-1}) and the vibrational band (39 cm^{-1}), thereby satisfying the criteria for strong coupling. In addition, as will be shown later, such new vibrational polaritonic bands are dispersive due to the optical component of the hybrid state.

Figure 2b shows the results obtained for a benzonitrile solution, which has several vibrational peaks (black curve), and the cavity was adjusted so that more than one mode is strongly coupled, as can be seen in the red spectrum. The cyanide group (CN) has a stretching frequency at 2229 cm^{-1}, which is split into two new peaks at 2260 and 2206 cm^{-1}, in other words with a Rabi splitting of 54 cm^{-1}. The smaller splitting as compared with DPPA is probably due to both the lower absorption and the smaller fwhm of the bare vibrational mode. Interestingly, at ~1500 cm^{-1}, the two aromatic C═C modes are close to each other and are coupled to the same optical mode, revealing a double splitting that will be discussed again later. Similarly the two C–C stretching bands at 758 and 687 cm^{-1} are simultaneously coupled to the bare cavity mode at 733 cm^{-1}.

The vibrational spectrum of citronellal is shown in Figure 2c. The Rabi splitting of the C═O stretch at 1726 cm^{-1} is 80 cm^{-1}. A very similar molecule, hexanal (not shown), has a C═O Rabi splitting of 105 cm^{-1}. Table 1 below summarizes our VSC findings for the different functional groups of the neat molecular liquids investigated. Before commenting on this Table, it is important to show the dispersion of the VSC. All of the strongly coupled vibrational bands are dispersive, as expected. Figure 3a illustrates this behavior for benzonitrile around two cavity modes that are involved in VSC: one that splits the CN stretching mode and the other involving the two aromatic C═C vibrations in a multiple splitting. Figure 3a shows how the spectra evolve with angle, and Figure 3b shows the corresponding dispersion curves derived from the peak positions (dots) of the transmission spectra. The experimental points are superimposed on the simulated curves calculated from the transfer-matrix approach, showing excellent agreement. The clear dispersion of the modes shows the light-matter hybrid nature of the new states generated under strong coupling. The double splitting involving the two C═C aromatic stretching modes is reminiscent of the coupling of two closely spaced electronic transitions to the same optical mode observed when two different molecules are located inside the same cavity.[40] Upon increasing incidence angle, the cavity

DOI: 10.1021/acs.jpclett.5b00204
J. Phys. Chem. Lett. 2015, 6, 1027–1031

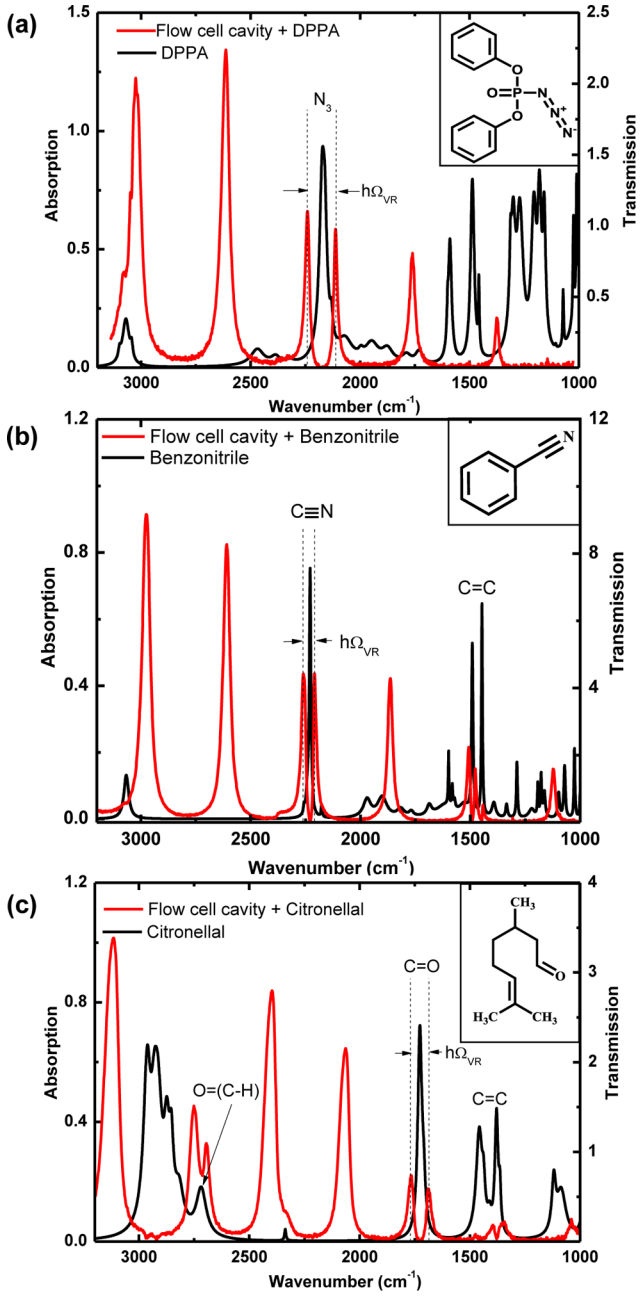

Figure 2. IR absorption spectra of three different molecules (black curves in absorption) and their transmission spectra under strong coupling with the Fabry–Perot cavity modes (red curves in transmission): (a) diphenyl phosphoryl azide (DPPA), (b) benzonitrile, and (c) citronellal.

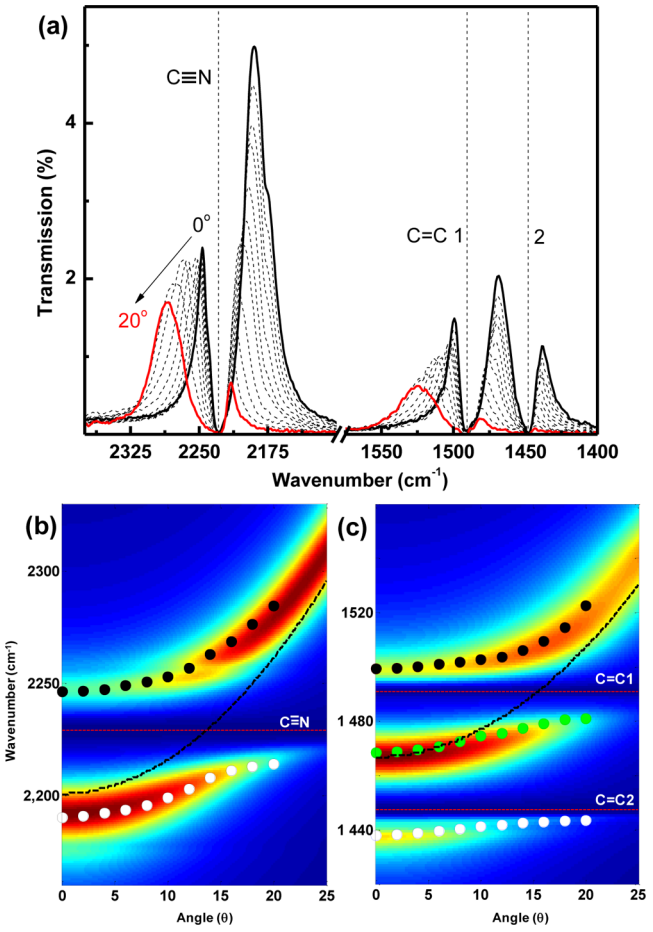

Figure 3. (a) Transmission spectra for different incidence angles (0–20°) of two cavity modes coupled with the CN and C=C stretching bands of benzonitrile. (b,c) Dispersion color plots for CN and C=C stretching bands, respectively. The cavity mode around 2200 cm^{-1} (normal incidence) moves in the dispersion curve and is strongly coupled to the CN stretch at 2230 cm^{-1} (14° incidence angle). The cavity mode cal. 1470 cm^{-1} (as shown in panel c) is doubly coupled to the two C=C stretching modes at normal incidence and selectively split the C=C (1) mode at 1491 cm^{-1} with higher angle of incidence. The dashed black line represents the dispersion of the calculated uncoupled cavity modes, and the dashed red line is the fixed vibration frequencies of interacting bands.

mode moves to higher energies, reaching the resonance point with the C=C (1) around 15°. At this point, the upper two hybrid modes will mainly have the properties of the pure cavity mode and the C=C (1) vibrational band, while the lowest C=

Table 1. Vibrational Rabi Splittings for Various Molecular Liquids

compound	conc. (M)	band assignment	band position (cm^{-1})	extinction by integrated absorption (10^3 cm^{-2} M^{-1})	$\hbar\Omega_{VR}$ (cm^{-1})
DPPA	4.65	(N=N=N)	2169	12.62	127
benzonitrile	9.7	(C=N)	2229	1.14	54
		aro. (C=C) (1)	1491	0.66	22[a]
		aro. (C=C) (2)	1447	0.60	26[a]
citronellal	5.54	(C=O)	1726	5.46	80
		(C=C) (1)	1456	3.58	60[a]
		(C=C) (2)	1379	2.16	52[a]
hexanal	8.14	(C=O)	1727	7.74	105

[a]Calculated values after removing the effects of neighboring bands in the simulation.

DOI: 10.1021/acs.jpclett.5b00204
J. Phys. Chem. Lett. 2015, 6, 1027–1031

C (2) band is very weakly coupled to the cavity mode, as can be seen from the weakly dispersive lowest branch at this region.

Table 1 shows the Rabi splitting observed for various bands in different molecules together with pertinent information. To assess the correlation between the splitting for each of the vibrational bands and their physical properties, we calculated the integrated absorption coefficients of the different bonds versus the splitting observed in the experiments. One can clearly see that the splitting scales with the integrated extinction coefficient, emphasizing the effect of the transition dipole moment on the interaction strength, as is pointed to in eq 1. To evaluate the intrinsic splitting for the bands that were involved in multiple splitting, we calculated the splitting by removing the effects of close neighbor bands via simulation using the best fit parameters of the cavity.

In principle fundamental vibrational modes have resonances that are independent of each other. In reality, they can also couple if they meet a number of criteria such as sharing of symmetry and a common atom and having similar frequencies.[42] Therefore, one could expect that the Rabi splitting of one vibration would affect other modes if they are already interacting. To be able to detect such a feature, both the strongly coupled bond and the adjacent bond in interaction must be detectable at the cavity frequencies. Citronellal presents the correct experimental conditions for the aldehyde (CHO) group, where the C−H and C═O stretching modes are sharing a common atom. The C−H is isolated and weak at 2715 cm^{-1} (Figure 2c, black curve); however, no noticeable shift could be detected within our experimental resolution, as shown in Figure 4. This is probably due to the big frequency difference between the two modes, ∼1000 cm^{-1}.

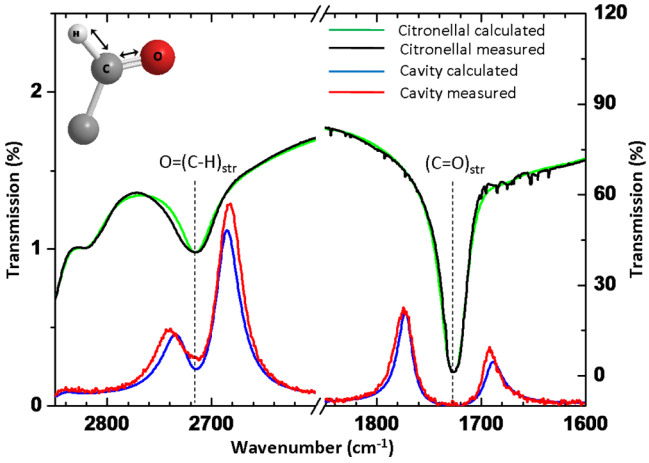

Figure 4. Measured (red) and calculated (blue) transmission spectra for pure citronellal solution inside the cavity. The inset shows 3D structure of the aldehyde functional group. The measured (black) and calculated (green) transmission spectra of the bare citronellal solution showing the bands of interest.

We have shown here for the first time that liquid-phase VSC can be easily achieved for a variety of functional groups in the IR as long as the absorption of the peaks are sufficiently strong to overcome the dephasing time associated with the components undergoing strong coupling. One or more vibrational modes of a molecule can be coupled simultaneously. While a vibrational frequency shift of a neighboring bond to that undergoing strong coupling could not be observed under our conditions, the collective mechanical oscillations of a large number of bonds of an ensemble of molecules nevertheless opens interesting perspectives with both fundamental and practical consequences. For molecular and material science, it confirms other studies that strong coupling can be used to change their properties in a significant and unique way by the perturbation of the energy levels of each molecule, the formation of the collective extended hybrid light-matter states involving many molecules, and the introduction of a dispersive quality to properties. These features combined with the possibility to do this in solution, as shown here, open many exciting possibilities such as the site-selective chemistry by softening a given bond targeted for reaction.

METHODS

All of the compounds used for the studies were purchased from Sigma-Aldrich (analytical grade). The liquid sample cell unit was purchased from Specac, and to obtain a Fabry−Perot cavity, we coated ZnSe windows with Au (10 nm) film, sandwiched by Mylar spacers. The spectra of the cavity were acquired by standard FTIR (Fourier transform infrared) spectrometer (Nicolet 6700) in transmission mode. The transmission was collected by DTGS (deuterated triglycine sulfate) detector with 0.5 cm^{-1} resolution and 32 scans. The dispersion curves were acquired by changing the incidence angle outside the cavity in the range 0−20° by steps of 2°, where the divergence at the waist of the beam is <2°, as estimated from the theoretical fit. The vibrational bands of the species studied in this work were modeled using the Lorentz−Lorenz model for multiple damped oscillators, and the metallic mirrors optical properties were modeled using the Drude−Lorenz model. The theoretical fit of the experimental measurements was performed using the standard propagation matrices approach for light in homogeneous and isotropic stratified media.[41]

AUTHOR INFORMATION

Corresponding Author

*E-mail: ebbesen@unistra.fr.

Notes

The authors declare no competing financial interest.

ACKNOWLEDGMENTS

This work was supported in part by the ERC "Plasmonics" no 22577, the ANR Equipex "Union" (ANR-10-EQPX-52-01), the Labex NIE projects (ANR-11-LABX-0058_NIE), and USIAS within the Investissement d'Avenir program ANR-10-IDEX-0002-02.

REFERENCES

(1) Pockrand, I.; Brillante, A.; Möbius, D. Exciton−Surface Plasmon Coupling: An Experimental Investigation. *J. Phys. Chem.* **1982**, *77*, 6289−6295.

(2) Fujita, T.; Sato, Y.; Kuitani, T.; Ishihara, T. Tunable Polariton Absorption of Distributed Feedback Microcavities at Room Temperature. *Phys. Rev. B* **1998**, *57*, 12428−12434.

(3) Lidzey, D. G.; Bradley, D. D. C.; Skolnick, M. S.; Virgili, T.; Walker, S.; Whittaker, D. M. Strong Exciton−Photon Coupling in an Organic Semiconductor Microcavity. *Nature* **1998**, *395*, 53−55.

(4) Song, J. H.; He, Y.; Nurmikko, A. V.; Tischler, J.; Bulovic, V. Exciton-Polariton Dynamics in a Transparent Organic Semiconductor Microcavity. *Phys. Rev. B* **2004**, *69*, 235330.

DOI: 10.1021/acs.jpclett.5b00204
J. Phys. Chem. Lett. 2015, 6, 1027−1031

(5) Wiederrecht, G. P.; Hall, J. E.; Bouhelier, A. Control of Molecular Energy Redistribution Pathways Via Surface Plasmon Gating. *Phys. Rev. Lett.* **2007**, *98*, 083001.
(6) Berrier, A.; Cools, R.; Arnold, C.; Offermans, P.; Crego-Calama, M.; Brongersma, S. H.; Gomez-Rivas, J. Active Control of the Strong Coupling Regime between Porphyrin Excitons and Surface Plasmon Polaritons. *ACS Nano* **2010**, *5*, 6226−6232.
(7) Kéna-Cohen, S.; Forrest, S. R. Room-Temperature Polariton Lasing in an Organic Single-Crystal Microcavity. *Nat. Photonics* **2010**, *4*, 371−375.
(8) Plumhof, J. D.; Stöferle, T.; Mai, L.; Scherf, U.; Mahrt, R. F. Room-Temperature Bose−Einstein Condensation of Cavity Exciton−Polaritons in a Polymer. *Nat. Mater.* **2014**, *13*, 247−252.
(9) Schwartz, T.; Hutchison, J. A.; Genet, C.; Ebbesen, T. W. Reversible Switching of Ultrastrong Light-Molecule Coupling. *Phys. Rev. Lett.* **2011**, *106*, 196405.
(10) Shalabney, A.; George, J.; Hutchison, J. A.; Pupillo, G.; Genet, C.; Ebbesen, T. W. Coherent Coupling of Molecular Resonators with a Microcavity Mode. arXiv:1403.1050 [quant-ph], March 5, 2014; idem. *Nat. Commun.* **2015**, *6*, 5981.
(11) Hayashi, S.; Ishigaki, Y.; Fujii, M. Plasmonic Effects on Strong Exciton-Photon Coupling in Metal-Insulator-Metal Microcavities. *Phys. Rev. B* **2012**, *86*, 045408.
(12) Schwartz, T.; Hutchison, J. A.; Léonard, J.; Genet, C.; Haacke, S.; Ebbesen, T. W. Polariton Dynamics under Strong Light−Molecule Coupling. *ChemPhysChem* **2013**, *14*, 125−131.
(13) Wang, S.; Chervy, T.; George, J.; Hutchsion, J. A.; Genet, C.; Ebbesen, T. W. Quantum Yield of Polariton Emission from Hybrid Light-Matter States. *J. Phys. Chem. Letters* **2014**, *5*, 1433−1439.
(14) Hutchison, J. A.; Schwartz, T.; Genet, C.; Devaux, E.; Ebbesen, T. W. Modifying Chemical Landscapes by Coupling to Vacuum Fields. *Angew. Chem., Int. Ed.* **2012**, *51*, 1592−1596.
(15) Hutchison, J. A.; Liscio, A.; Schwartz, T.; Canaguier-Durand, A.; Genet, C.; Palermo, V.; Samorì, P.; Ebbesen, T. W. Tuning the Work-Function via Strong Coupling. *Adv. Mater.* **2013**, *25*, 2481−2485.
(16) Fontcuberta i Morral, A.; Stellacci, F. Light-Matter Interactions: Ultrastrong Routes to New Chemistry. *Nat. Mater.* **2012**, *11*, 272−273.
(17) Wang, S.; Mika, A.; Hutchsion, J. A.; Genet, C.; Jouaiti, A.; Hosseini, M. W.; Ebbesen, T. W. Phase Transition of a Perovskite Strongly Coupled to the Vacuum Field. *Nanoscale* **2014**, *6*, 7243−7248.
(18) Orgiu, E.; et al. Conductivity in Organic Semiconductors Mediated by Polaritonic States. arXiv:1409.1900 [cond-mat.mtrl-sci], September 5, 2014.
(19) Dintinger, J.; Klein, S.; Bustos, F.; Barnes, W. L.; Ebbesen, T. W. Strong Coupling between Surface Plasmon-Polaritons and Organic Molecules in Subwavelength Hole Arrays. *Phys. Rev. B* **2005**, *71*, 035424.
(20) Canaguier-Durand, A.; Devaux, E.; George, J.; Pang, Y.; Hutchison, J. A.; Schwartz, T.; Genet, C.; Wilhelms, N.; Lehn, J.-M.; Ebbesen, T. W. Thermodynamics of Molecules Strongly Coupled to the Vacuum Field. *Angew. Chem., Int. Ed.* **2013**, *52*, 10533−10536.
(21) Canaguier-Durand, A.; Genet, C.; Lambrecht, A.; Ebbesen, T. W.; Reynaud, S. Non-Markovian Polariton Dynamics in Organic Strong Coupling. *Eur. Phys. J. D* **2015**, *69*, 24.
(22) Vasa, P.; Pomraenke, R.; Cirmi, G.; De Re, E.; Wang, W.; Schwieger, S.; Leipold, D.; Lienau, C. Ultrafast Manipulation of Strong Coupling in Metal−Molecular Aggregate Hybrid Nanostructures. *ACS Nano* **2010**, *42*, 7559−7565.
(23) Salomon, A.; Wang, S.; Hutchison, J. A.; Genet, C.; Ebbesen, T. W. Strong Light-Molecule Coupling on Plasmonic Arrays of Different Symmetry. *ChemPhysChem* **2013**, *14*, 1882−1886.
(24) Koponen, M. A.; Hohenester, U.; Hakala, T. K.; Toppari, J. J. Absence of Mutual Polariton Scattering for Strongly Coupled Surface Plasmon Polaritons and Dye Molecules with a Large Stokes Shift. *Phys. Rev. B* **2013**, *88*, 085425.
(25) Ni, W.; Yang, Z.; Chen, H.; Li, L.; Wang, J. Coupling Between Molecular and Plasmonic Resonances in Freestanding Dye−Gold Nanorod Hybrid Nanostructures. *J. Am. Chem. Soc.* **2008**, *130*, 6692−6693.
(26) Gómez, D. E.; Lo, S. S.; Davis, T. J.; Hartland, G. V. Picosecond Kinetics of Strongly Coupled Excitons and Surface Plasmon Polaritons. *J. Phys. Chem. B* **2012**, *117*, 4340−4346.
(27) Zengin, G.; Johansson, G.; Johansson, P.; Antosiewicz, T. J.; Käll, M.; Shegai, T. Approaching the Strong Coupling Limit in Single Plasmonic Nanorods Interacting with J-Aggregates. *Sci. Rep.* **2013**, *3*, 3074.
(28) Nagasawa, F.; Takase, M.; Murakoshi, K. Raman Enhancement via Polariton States Produced by Strong Coupling between a Localized Surface Plasmon and Dye Excitons at Metal Nanogaps. *J. Phys. Chem. Lett.* **2014**, *5*, 14−19.
(29) Zhu, Y.; Gauthier, D. J.; Morin, S. E.; Wu, Q.; Carmichael, H. J.; Mossberg, T. W. Vacuum Rabi Splitting as a Feature of Linear-Dispersion Theory: Analysis and Experimental Observations. *Phys. Rev. Lett.* **1990**, *64*, 2499−2502.
(30) Gambino, S.; et al. Exploring Light−Matter Interaction Phenomena under Ultrastrong Coupling Regime. *ACS Photonics* **2014**, *1*, 1042−1048.
(31) Marinica, D. C.; Lourenço-Martins, H.; Aizpurua, J.; Borisov, A. G. Plexciton Quenching by Resonant Electron Transfer from Quantum Emitter to Metallic Nanoantenna. *Nano Lett.* **2013**, *13*, 5972−5978.
(32) Väkeväinen, A. I.; Moerland, R. J.; Rekola, H. T.; Eskelinen, A.-P.; Martikainen, J.-P.; Kim, D.-H.; Törmä, P. Plasmonic Surface Lattice Resonances at the Strong Coupling Regime. *Nano Lett.* **2014**, *14*, 1721−1727.
(33) Shi, L.; Hakala, T. K.; Rekola, H. T.; Martikainen, J.-P.; Moerland, R. J.; Törmä, P. Spatial Coherence Properties of Organic Molecules Coupled to Plasmonic Surface Lattice Resonances in the Weak and Strong Coupling Regimes. *Phys. Rev. Lett.* **2014**, *112*, 153002.
(34) Antosiewicz, T. J.; Peter-Apell, S.; Shegai, T. Plasmon−Exciton Interactions in a Core−Shell Geometry: From Enhanced Absorption to Strong Coupling. *ACS Photonics* **2014**, *1*, 454−463.
(35) Gómez, D. E.; Giessen, H.; Davis, T. J. Semiclassical Plexcitonics: Simple Approach for Designing Plexcitonic Nanostructures. *J. Phys. Chem. C* **2014**, *118*, 23963−23969.
(36) Herrera, F.; Peropadre, B.; Pachon, L. A.; Saikin, S. K.; Aspuru-Guzik, A. Quantum Nonlinear Optics with Polar J-Aggregates in Microcavities. *J. Phys. Chem. Lett.* **2014**, *5*, 3708−3715.
(37) Karademir, E.; Balci, S.; Kocabas, C.; Aydinli, A. Plexcitonic Crystals: A Tunable Platform for Light-Matter Interactions. *Opt. Express* **2014**, *22*, 21912.
(38) Törmä, P.; Barnes, W. L. Strong Coupling between Surface Plasmon Polaritons and Emitters: A Review. *Rep. Prog. Phys.* **2015**, *78*, 013901.
(39) Zengin, G.; Johansson, G.; Johansson, P.; Antosiewicz, T. J.; Käll, M.; Shegai, T. Approaching the Strong Coupling Limit in Single Plasmonic Nanorods Interacting with J-Aggregates. *Sci. Rep.* **2013**, *3*, 3074.
(40) Lidzey, D. G.; Bradley, D. D. C.; Armitage, A.; Walker, S.; Skolnick, M. S. Photon-Mediated Hybridization of Frenkel Excitons in Organic Semiconductor Microcavities. *Science* **2000**, *288*, 1620.
(41) Shalabney, A.; Abdulhalim, I. Electromagnetic Fields Distribution in Multilayer Thin Film Structures and the Origin of Sensitivity Enhancement in Surface Plasmon Resonance Sensors. *Sens. Actuators, A* **2010**, *159*, 24−32.
(42) Silverstein, R. M.; Basler, G. C.; Morill, T. C. Chapter 3. In *Spectrometric Identification of Organic Compounds*; John Wiley & Sons, Inc.: Hoboken, NJ, 1991.

DOI: 10.1021/acs.jpclett.5b00204
J. Phys. Chem. Lett. 2015, 6, 1027−1031